Dual Templating Synthesis of Mesoporous Titanium Nitride Microspheres

By *Jin Ho Bang* and *Kenneth S. Suslick**

Dedicated to Prof. Theodore L. Brown on the happy occasion of his 80th birthday

The synthesis of new porous materials remains an exciting area of research, in part because of their potential use in diverse applications.[1] Materials having hierarchically porous nanostructures (such as bimodal mesoporous, meso–macroporous, or mesoporous–hollow materials) are particularly intriguing because they can uncouple overall mass transport from the chemical and physical properties of the finer pore structure.[2] The general synthetic methodology for hierarchically porous nanostructures has relied heavily on the use of multiple sacrificial templates (amphiphilic micellar scaffolds, block copolymers, colloidal silica, or polymer spheres)[1–3] as components of a preliminary nanocomposite. Thus, post-treatments (chemical etching or thermal heat-treatment) must be used to render the various nanostructured porosities in the final products. Despite the usefulness of such templates, they inherently require the use of prestructured templates (which are relatively expensive) and the necessity of post-processing removal of the template (which is generally cumbersome, hazardous, or incomplete). There remains, therefore, an urgent need for new synthetic methods that do not require an externally added sacrificial template. In addition, there have been few attempts to prepare the hierarchically porous nanostructures of non-oxide materials such as metal nitrides and carbides (TiN, Si_3N_4, F or Mo_2C). Metal nitrides and carbides have substantial advantages in high-temperature catalysis, including higher melting points, lower sintering tendencies, and greater chemical inertness under non-oxidizing conditions.[4]

We have therefore developed a new and general route to the preparation of hierarchically porous nanostructures of refractory nitrides that avoids the use of external sacrificial templates. Here, we report an ultrasonic spray pyrolysis (USP) preparation of hierarchically nanostructured titanium nitride (TiN) using an in situ dual templating from an initial soft liquid-core template and second from the resulting hard binary-oxide shell. In our new synthetic approach, multimodal porous nanostructures (mesoporous and hollow macroporous) are obtained without the use of any prestructured templates or any additional template-removing procedures.

[*] Prof. K. S. Suslick, J. H. Bang
School of Chemical Sciences
University of Illinois at Urbana-Champaign
600 South Mathews Avenue
Urbana, Illinois 61801 (USA)
E-mail: ksuslick@uiuc.edu

DOI: 10.1002/adma.200802309

TiN is a hard, electrically conductive, and wear- and corrosion-resistive material that has been used in the microelectronic industry as a conductive diffusion barrier.[5] Recent reports have found its potential use in various other applications, such as catalysis, hydrogen storage, supercapacitors, pH sensors, electroanalysis, etc.[5,6] In general, TiN powder is prepared by firing Ti metal or TiO_2 under ammonia gas as a nitrogen source.[5b,7] Several attempts have been made toward the preparation of nanostructured TiN,[5a,6a,7b,8,9] but none have succeeded in creating a simple and facile synthetic route to hierarchically porous nanostructures of TiN.

Recently, ultrasonic spray pyrolysis (USP) has achieved significant prominence for the synthesis of various nanostructured materials, including metal sulfides, oxides, and carbons.[10] Because of its unique operation conditions (continuous production of sub-micrometer microreactors, that is, isolated droplets in a hot-gas stream), USP stands out from other various synthetic routes (which are all essentially batch reactions in macroscale reactors) in the preparation of nanocomposite materials. The success of recent USP syntheses in preparing hollow or porous materials has generally still relied on sacrificial-template materials (colloidal silica or polymer spheres) as one of the components of the nanocomposites,[10c–f,h,k] which then require post-treatment to produce the final porous structures. There have been some efforts to address this issue, such as the use of water-soluble metal salts (NaCl or LiCl) as the second component of nanocomposites.[10b,i]

In order to generate porous TiN, we decided to use zinc titanate (Zn_2TiO_4) as a precursor from which we discovered we could remove Zn during nitration with ammonia, as outlined in Figure 1. We therefore used USP of an aqueous solution containing a simple Zn salt (zinc nitrate hexahydrate, $Zn(NO_3)_2 \cdot 6H_2O$) and a soluble Ti(IV) complex ($[NH_4]_2$ [$Ti^{IV}(OH)_2(OCH(CH_3)CO_2)_2$]) to obtain zinc titanate. This Ti(IV) complex was specifically chosen because it does not readily hydrolyze to TiO_2; indeed, it is stable at room temperature approximately between pH 2 and pH 10.[11] To our surprise, the products so obtained were *not* solid particles, but rather hollow spheres of zinc titanate (Zn_2TiO_4), as shown in Figure 2a and b (see Fig. S1 in Supporting Information (SI) for more electron microscopy images of Zn_2TiO_4). The formation of the hollow spheres was further confirmed by energy-dispersive X-ray spectroscopy (EDS) line analysis and elemental mapping analysis, respectively (Figs. S2 and S3 in SI).

The final TiN powder obtained after the nitration of hollow Zn_2TiO_4 spheres exhibited a dramatic change in morphology and

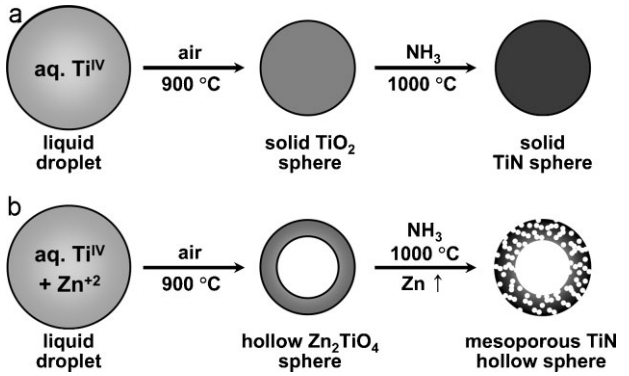

Figure 1. Schematic of a) conventional USP-assisted synthesis of TiN solid spheres and b) in situ dual templating synthesis of mesoporous TiN microspheres. Aq. Ti^{IV} refers to a 50% aqueous solution of the Ti^{IV} precursor complex, $[NH_4]_2[Ti^{IV}(OH)_2(OCH(CH_3)CO_2)_2]$.

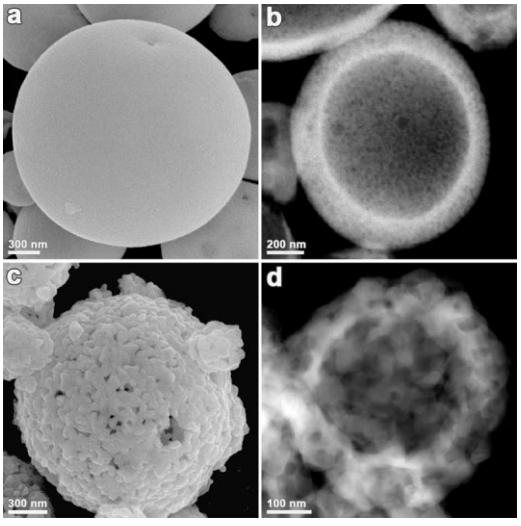

Figure 2. SEM and TEM images of a Zn_2TiO_4 hollow sphere (a and b, respectively) and mesoporous TiN microspheres (c and d, respectively).

pore structure: hollow macroporous core and mesoporous shell, as shown in Figure 2c and d (see Figs. S4–S6 in SI for more electron microscopy images and EDS analysis of TiN). High-resolution transmission electron microscopy (TEM) was used to examine the pore structure created during the heat-treatment, and showed that the shell of TiN hollow spheres was perforated with a random network of mesopores (Fig. S6 in SI). The generation of the mesoporosity during the NH_3 heat-treatment was also verified by N_2-sorption isotherm measurement. Figure 3a shows that the mesoporous TiN microspheres exhibit a typical type-IV isotherm, characteristic of mesoporous materials, with the Brunauer–Emmett–Teller (BET) surface area of 17 $m^2 g^{-1}$. Pore-size distribution obtained using the Barrett–Joyner–Halenda (BJH) method (Fig. 3b) reveals that the majority of pores are larger than 15 nm with a maximum at 20 nm, in good agreement with TEM. X-ray diffraction (XRD) patterns obtained before and after the NH_3 heat-treatment manifest the creation of Zn_2TiO_4 via USP and the conversion of Zn_2TiO_4 to TiN through the following nitration (Fig. 4).

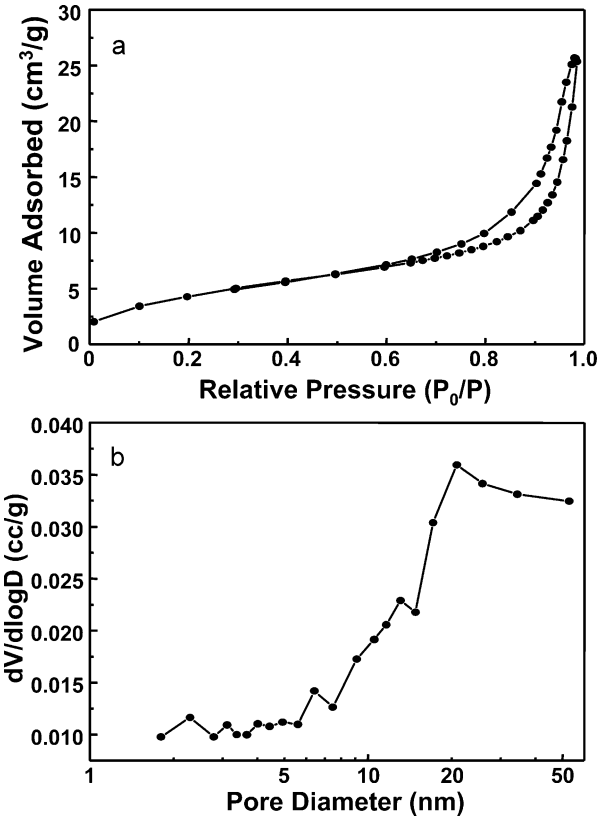

Figure 3. a) Nitrogen adsorption and desorption isotherms of mesoporous TiN microspheres and b) their pore-size distribution obtained from adsorption branch of the isotherm using the BJH method.

As a control, USP of the same aqueous solution of the Ti(IV) complex ($[NH_4]_2[Ti^{IV}(OH)_2(OCH(CH_3)CO_2)_2]$) in the absence of Zn salts produced TiO_2 solid spheres, which were then nitrated by heat-treatment under ammonia flow, as illustrated in Figure 1a. The TiO_2 solid spheres from USP were a few micrometers in diameter and had a smooth surface, and the TiN obtained after the NH_3 heat-treatment maintained its original spherical morphology, but with a roughened surface (see Fig. S7–S9 in SI for characterization). The final particle size can be predicted and controlled as a function of the initial concentration of precursors in the volatile solvent (in this case, water) and of the droplet size in the ultrasonic mist, which itself is controlled by the ultrasonic frequency and surface tension of the nebulized solution.[12]

In order to investigate the origin of the unusual mesoporous TiN formed from our Zn_2TiO_4 spherical shells, we first examined decomposition pathways of both precursors using thermogravimetric analysis (TGA) and differential scanning calorimetry (DSC). Figure 5 shows the TGA/DSC analysis of $Zn(NO_3)_2 \cdot 6H_2O$ and $[NH_4]_2[Ti^{IV}(OH)_2(OCH(CH_3)CO_2)_2]$, respectively. Thermal decomposition of $Zn(NO_3)_2 \cdot 6H_2O$ starts with melting (or more accurately, dissolving into its own solvate water) at 36 °C, followed by several steps of water loss, and the decomposition of anhydrous $Zn(NO_3)_2$ from ≈300 °C to ≈340 °C. In comparison, the titania precursor shows water loss and decomposition followed by condensation of OH groups. Notably, $Zn(NO_3)_2 \cdot 6H_2O$ finishes its decomposition before the complete decomposition/

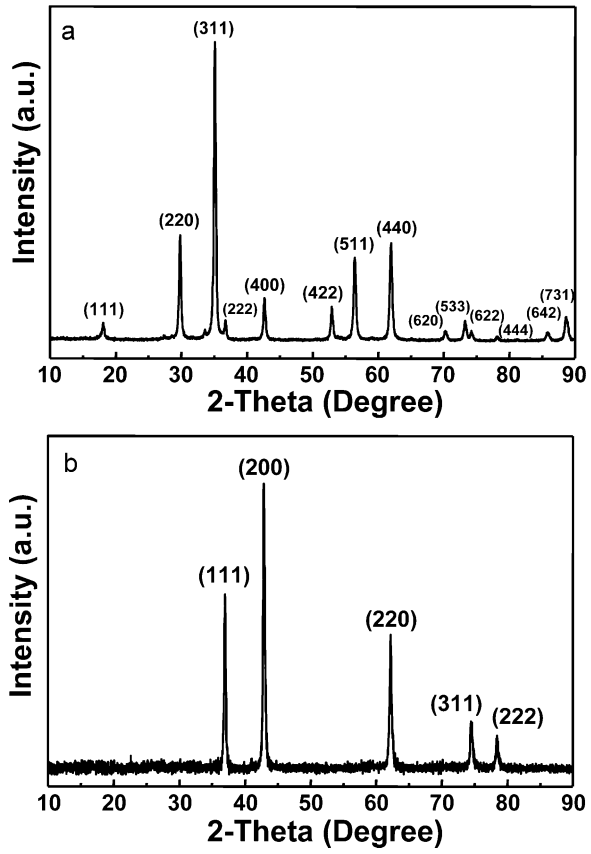

Figure 4. XRD patterns of a) Zn_2TiO_4 hollow spheres and b) mesoporous TiN hollow spheres.

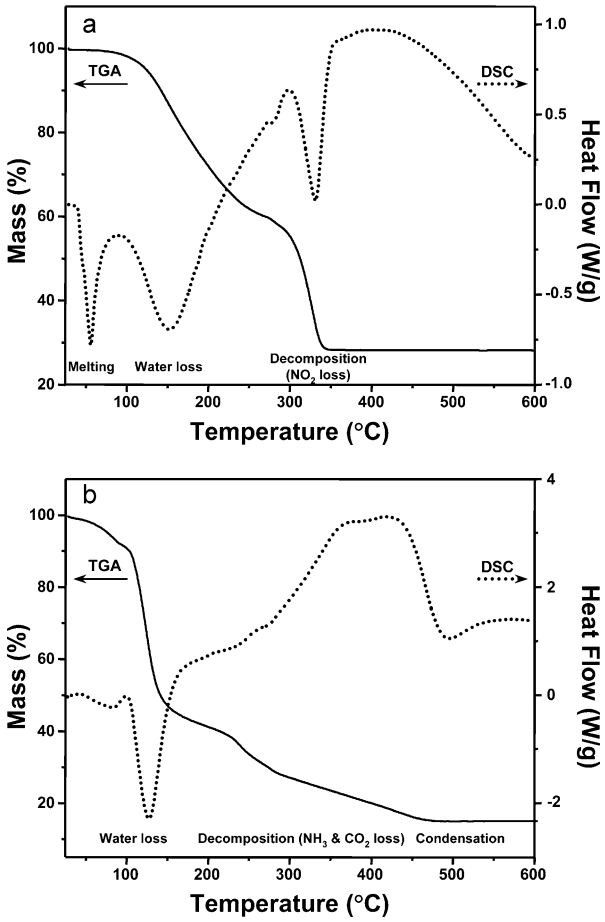

Figure 5. TGA/DSC analysis of a) $Zn(NO_3)_2 \cdot 6H_2O$ and b) 50 wt% water solution of $[NH_4]_2[Ti^{IV}(OH)_2(OCH(CH_3)CO_2)_2]$ (diammonium dihydroxo-dilactatotitanate(IV) (2–).

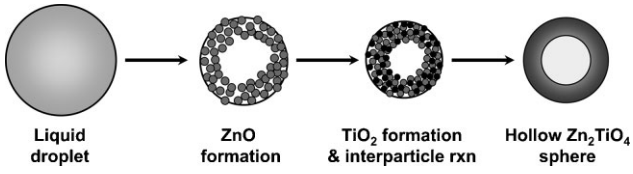

Figure 6. Schematic of hollow Zn_2TiO_4 sphere formation.

condensation of the titania precursor; as discussed below, we believe that this order of decomposition reactions plays an important role in the formation of hollow spheres of Zn_2TiO_4.

During spray pyrolysis, when a precursor melts before decomposition, hollow porous spheres often result. Decomposition of the molten precursor droplets so formed generally results in the formation of a solid shell surrounding the initially liquid precursor core.[12] This hollow shell may undergo several possible transformations: it may remain a rigid hollow sphere or it may shrivel into a raisin-like shell or burst open or collapse, depending of the formation of gases upon precursor decomposition and the nature of any further densification of the shell.[12]

We suggest that the intermediate hollow solid shell of ZnO first formed during the heating process retains its structural integrity and serves as an in situ template for the hollow Zn_2TiO_4 sphere formation. The decomposition of $Zn(NO_3)_2 \cdot 6H_2O$ occurs before the titania precursor completely decomposes, and the resulting structure of ZnO serves as a hollow scaffold on which the titania precursor reacts to produce Zn_2TiO_4, as illustrated in Figure 6. Of direct relevance to this proposed mechanism, the USP of $Zn(NO_3)_2 \cdot 6H_2O$ does indeed produce a porous and hollow sphere of ZnO, as confirmed in control experiments (Fig. S10 in SI).[13]

Figure 7 presents EDS analysis of the hollow Zn_2TiO_4 spheres before and after the NH_3 heat-treatment. Prior to the heat-treatment, intense Zn signals were observed along with Ti and O peaks. After exposure to NH_3, however, Zn is no longer present in the EDS analysis. This result clearly shows that zinc and its oxygen counterions were etched out during the nitration process. In order to elucidate the etching mechanism, a dark powder collected from the downstream wall of a quartz tube after the nitration was analyzed by XRD (Fig. 8). The resolved diffraction peaks of the powder match the standard Zn metal sample (JCPDS 04-0831), together with trace ZnO peaks (presumably from oxidation on the Zn metal surface). No evidence of the formation of zinc nitride was observed in XRD analysis, which was confirmed with XPS analysis that showed no nitrogen peak (Fig. S11 in SI).

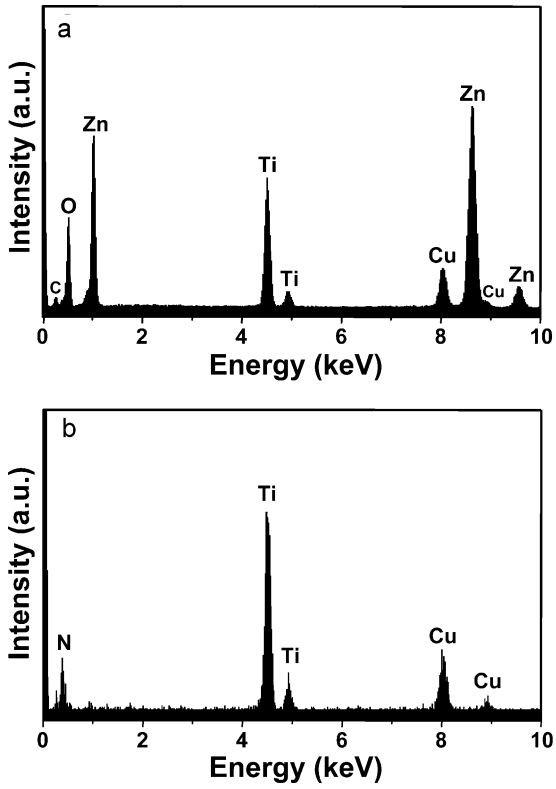

Figure 7. TEM-EDS of Zn_2TiO_4 hollow spheres a) before and b) after heat-treatment under NH_3 atmosphere (C and Cu signals from the TEM sample grid).

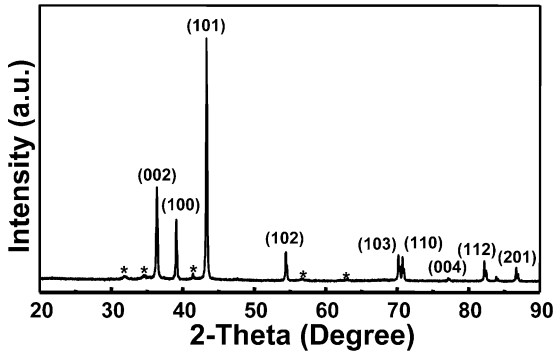

Figure 8. XRD pattern of Zn metal deposited on the downstream wall of a quartz tube during NH_3 heat-treatment (traces of ZnO, labeled as asterisks, were observed probably due to surface oxidation).

The creation of mesopores in the TiN shell is attributed to the chemical etching of Zn and its oxygen counterions during the nitration with NH_3. It is known that ZnO can be reduced to Zn metal under a hot ammonia-gas flow (Eq. 1).[14] On the basis of XRD, XPS, and electron microscopy, we conclude that Zn atoms (which initially occupy the tetrahedral and octahedral sites of the inverse spinel oxide lattice of Zn_2TiO_4)[15] were reduced to Zn metal during the NH_3 heat-treatment, and the Zn metal was evaporated from the shell of the microsphere due to its low boiling point (907 °C). It is the evaporative loss of the Zn, N_2, and H_2O during this process (Eq. 1) that creates the mesopores into the TiN shell.

$$3ZnO + 2NH_3 \rightarrow 3Zn + N_2 + 3H_2O \quad (1)$$

Similar, Zn leaching using high-temperature H_2 reduction to create mesopores or a hollow interior were previously reported in the preparation of GaN[16] and metal oxides.[17] In these cases, ZnO was reduced to Zn metal by hot H_2 gas, and subsequently evaporated out as Zn vapor. Our results, however, are the first demonstration of Zn removal by hot anhydrous NH_3 gas.

In summary, we demonstrated in situ dual templating in the preparation of a hierarchically nanostructured material. Our synthesis of mesoporous TiN hollow microspheres utilizes no external prestructured template (nor removal of the same), but rather involves the formation during USP of hollow Zn_2TiO_4 spheres as a TiN precursor, followed by high temperature nitration under an ammonia atmosphere, which creates the mesoporosity. For such dual templating, it is essential to have precursors that decompose sequentially (the second precursor component should have a higher decomposition temperature than zinc nitrate). Given that precondition, this novel synthetic route can be further extended to the preparation of other hierarchically nanostructured metal nitrides and even metal oxides (if H_2 reduction is employed for Zn etching).

Experimental

Mesoporous TiN microspheres were prepared by nitration of hollow Zn_2TiO_4 spheres obtained using USP. For the preparation of hollow Zn_2TiO_4 spheres, a household humidifier operating at 1.7 MHz (Sunbeam model no. 696) nebulized an aqueous precursor solution composed of 180 mM zinc nitrate hexahydrate ($Zn(NO_3)_2 \cdot 6H_2O$) and 85 mM diammonium dihydroxodilactatotitanium(IV) (2–) ($[NH_4]_2[Ti^{IV}(OH)_2(OCH(CH_3)CO_2)_2]$); both reagents were obtained from Sigma–Aldrich and used as received. Aerosol droplets produced by the nebulization were carried through a furnace at 900 °C by air flow at a rate of 1 standard liter per minute (SLPM). As the droplets passed through the furnace, the precursor decomposed and produced fine particles, which were collected in a series of bubblers containing deionized water. The product was isolated from collection media by centrifugation, washed with deionized water several times, and dried at room temperature. To prepare the mesoporous hollow spheres of TiN, the dried Zn_2TiO_4 powder was heat-treated at 1000 °C under anhydrous NH_3 gas flow (0.5 L min^{-1}) for 2 h. As a control experiment, a solution containing 85 mM diammonium dihydroxodilactatotitanium(IV) (2–) was nebulized and decomposed under the same experimental conditions, and the product so obtained (TiO_2) was exposed to ammonia under the same heat-treatment conditions: solid TiN microspheres were the final result (Figs. S7–S9).

For characterization, scanning electron microscopy (SEM) was carried out using a Hitachi S-4700, and transmission electron microscopy (TEM) and scanning transmission electron microscopy (STEM) were conducted using a JEOL 2010F equipped with EDS (energy dispersive X-ray spectroscopy) detector (Oxford INCA 30 mm ATW detector) at an acceleration voltage of 200 kV. Powder X-ray diffraction (XRD) patterns were obtained using a Rigaku D-MAX diffractometer using a Cu Kα radiation. Nitrogen adsorption and desorption isotherms were measured using a Nova 2200e Surface Area and Pore Analyzer (Quantachrome Instruments) at −196 °C, and the specific surface area was determined according to the BET method. The pore-size distribution was analyzed using the BJH method with adsorption branch. TGA and DSC of zinc nitrate hexahydrate and diammonium dihydroxodilactatotitanium(IV) (2–) were carried out using a Netzsch simultaneous thermal analyzer

(STA 409 C/CD) with a temperature ramp of 10 °C min^{-1} under air flow. X-ray photoelectron spectroscopy (XPS) measurements were performed using a Kratos Axis-Ultra imaging X-ray photoelectron spectrometer.

Acknowledgements

We gratefully acknowledge Prof. W. M. Kriven and J. Bell for their generous assistance in TGA/DSC data acquisition. This material is based on work supported by the U.S. Department of Energy, Division of Materials Sciences under Award No. DE-FG02-07ER46418, through the Frederick Seitz Materials Research Laboratory at the University of Illinois at Urbana-Champaign. This research was carried out in part in the Center for Microanalysis of Materials, UIUC, which is partially supported by the U.S. Department of Energy under grant DE-FG02-07ER46418. Supporting Information is available online from Wiley InterScience or from the author.

Received: August 8, 2008
Published online:

[1] a) M. E. Davis, *Nature* **2002**, *417*, 813. b) G. J. de A. A. Soler-Illia, C. Sanchez, B. Lebeau, J. Patarin, *Chem. Rev.* **2002**, *102*, 4093. c) A. Stein, *Adv. Mater.* **2003**, *15*, 763. d) Y. Wan, Y. Shi, D. Zhao, *Chem. Commun.* **2007**, 897. e) M. G. Kanatzidis, *Adv. Mater.* **2007**, *19*, 1165. f) S. W. Boettcher, J. Fan, C.-K. Tsung, Q. Shi, G. D. Stucky, *Acc. Chem. Res.* **2007**, *40*, 784.

[2] a) Z.-Y. Yuan, B.-L. Su, *J. Mater. Chem.* **2006**, *16*, 663. b) P. Yang, T. Deng, D. Zhao, P. Feng, D. Pine, B. F. Chmelka, G. M. Whitesides, G. D. Stucky, *Science* **1998**, *282*, 2244. c) B. T. Holland, L. Abrams, A. Stein, *J. Am. Chem. Soc.* **1999**, *121*, 4308. d) M. W. Anderson, S. M. Holmes, N. Hanif, C. S. Cundy, *Angew. Chem. Int. Ed.* **2000**, *39*, 2707. e) J.-L. Blin, A. Léonard, Z.-Y. Yuan, L. Gigot, A. Vantomme, A. K. Cheetham, B.-L. Su, *Angew. Chem. Int. Ed.* **2003**, *42*, 2872. f) Z.-Y. Yuan, T.-Z. Ren, B.-L. Su, *Adv. Mater.* **2003**, *15*, 1462. g) G. S. S. Chai, I. S. Shin, J.-S. Yu, *Adv. Mater.* **2004**, *16*, 2057. h) K. Nakanishi, N. Tanaka, *Acc. Chem. Res.* **2007**, *40*, 863.

[3] A. Wolosiuk, O. Armagan, P. V. Braun, *J. Am. Chem. Soc.* **2005**, *127*, 16356.

[4] a) D. Farrusseng, K. Schlichte, B. Spliethoff, A. Wingen, S. Kaskel, J. S. Bradley, F. Schüth, *Angew. Chem. Int. Ed.* **2001**, *40*, 4204. b) S. Kaskel, K. Schlichte, *J. Catal.* **2001**, *201*, 270.

[5] a) R. A. Janes, M. Aldissi, R. B. Kaner, *Chem. Mater.* **2003**, *15*, 4431. b) M. Drygas, C. Czosnek, R. T. Paine, J. F. Janik, *Chem. Mater.* **2006**, *18*, 3122.

[6] a) S. Kaskel, K. Schlichte, T. Kratzke, *J. Mol. Catal. A* **2004**, *208*, 291. b) B. Bogdanović, M. Felderhoff, S. Kaskel, A. Pommerin, K. Schlichte, F. Schüth, *Adv. Mater.* **2003**, *15*, 1012. c) D. Choi, P. N. Kumta, *J. Electrochem. Soc.* **2006**, *153*, A2298. d) Y. Wang, H. Yuan, X. Lu, Z. Zhou, D. Xiao, *Electroanalysis* **2006**, *18*, 1493. e) C. N. Kirchner, K. H. Hallmeier, R. Szargan, T. Raschke, C. Radehaus, G. Wittstock, *Electroanalysis* **2007**, *19*, 1023. f) T. Nakayama, H. Wake, K. Ozawa, H. Kodama, N. Nakamura, T. Matsunaga, *Environ. Sci. Technol.* **1998**, *32*, 798. g) O. T. M. Musthafa, S. Sampath, *Chem. Commun.* **2008**, 67.

[7] a) S. H. Elder, F. J. DiSalvo, L. Topor, A. Navrotsky, *Chem. Mater.* **1993**, *5*, 1545. b) X. Z. Chen, J. L. Dye, H. A. Eick, S. H. Elder, K. L. Tsai, *Chem. Mater.* **1997**, *9*, 1172.

[8] A. Fischer, M. Antonietti, A. Thomas, *Adv. Mater.* **2007**, *19*, 264.

[9] S. Kaskel, K. Schlichte, G. Chaplais, M. Khanna, *J. Mater. Chem.* **2003**, *13*, 1496.

[10] a) P. Tartaj, T. González-Carreño, C. J. Serna, *Adv. Mater.* **2001**, *13*, 1620. b) B. Xia, W. Lenggoro, K. Okuyama, *Adv. Mater.* **2001**, *13*, 1579. c) F. Iskandar, A. Mikrajuddin, K. Okuyama, *Nano Lett.* **2001**, *1*, 231. d) F. Iskandar, A. Mikrajuddin, K. Okuyama, *Nano Lett.* **2002**, *2*, 389. e) S. E. Skrabalak, K. S. Suslick, *J. Am. Chem. Soc.* **2005**, *127*, 9990. f) W. H. Suh, K. S. Suslick, *J. Am. Chem. Soc.* **2005**, *127*, 12007. g) T. Zheng, J. Zhan, J. Pang, G. S. Tan, J. He, G. L. McPherson, Y. Lu, V. T. John, *Adv. Mater.* **2006**, *18*, 2735. h) W. H. Suh, A. R. Jang, Y.-H. Suh, K. S. Suslick, *Adv. Mater.* **2006**, *18*, 1832. i) S. E. Skrabalak, K. S. Suslick, *J. Am. Chem. Soc.* **2006**, *128*, 12642. j) J. H. Bang, K. Han, S. E. Skrabalak, H. Kim, K. S. Suslick, *J. Phys. Chem. C* **2007**, *111*, 10959. k) J. H. Bang, R. J. Helmich, K. S. Suslick, *Adv. Mater.* **2008**, *20*, 2599. l) J. H. Bang, W. H. Suh, K. S. Suslick, *Chem. Mater.* **2008**, *20*, 4033.

[11] a) A. Hanprasopwattana, T. Rieker, A. G. Sault, A. K. Datye, *Catal. Lett.* **1997**, *45*, 165. b) S. Baskaran, L. Song, J. Liu, Y. L. Chen, G. L. Graff, *J. Am. Ceram. Soc.* **1998**, *81*, 401. c) H. Möckel, M. Giersig, F. Willig, *J. Mater. Chem.* **1999**, *9*, 3051.

[12] a) G. L. Messing, S.-C. Zhang, G. V. Jayanthi, *J. Am. Ceram. Soc.* **1993**, *76*, 2707. b) E. G. Lierke, *Chem. Ing. Tech.* **1998**, *70*, 815. c) T. T. Kodas, M. J. Hampden-Smith, *Aerosol Processing of Materials*, Wiley-VCH, New York **1999**. d) P. S. Patil, *Mater. Chem. Phys.* **1999**, *59*, 185.

[13] C. Panatarani, I. W. Lenggoro, K. Okuyama, *J. Nanopart. Res.* **2003**, *5*, 47.

[14] a) Y. Yan, P. Liu, M. J. Romero, M. M. Al-Jassim, *J. Appl. Phys.* **2003**, *93*, 4807. b) J. Li, X. Chen, *Solid State Commun.* **2004**, *131*, 769.

[15] Y. Yang, X. W. Sun, B. K. Tay, J. X. Wang, Z. L. Dong, H. M. Fan, *Adv. Mater.* **2007**, *19*, 1839.

[16] J. Goldberger, R. He, Y. Zhang, S. Lee, H. Yan, H.-J. Choi, P. Yang, *Nature* **2003**, *422*, 599.

[17] a) E. S. Toberer, R. Seshadri, *Adv. Mater.* **2005**, *17*, 2244. b) E. S. Toberer, A. Joshi, R. Seshadri, *Chem. Mater.* **2005**, *17*, 2142. c) E. S. Toberer, J. D. Epping, B. F. Chmelka, R. Seshadri, *Chem. Mater.* **2006**, *18*, 6345.